Protein Expression and Purification 185 (2021) 105906

Contents lists available at ScienceDirect

Protein Expression and Purification

journal homepage: www.elsevier.com/locate/yprep

Improving the yield of recalcitrant Nanobodies® by simple modifications to the standard protocol

Christopher K. Kariuki [a,b,*], Stefan Magez [a,c,d]

[a] Laboratory of Cellular and Molecular Interactions (CMIM), Vrije Universiteit Brussels, Brussels, Belgium
[b] Department of Tropical and Infectious Diseases, Institute of Primate Research (IPR), Nairobi, Kenya
[c] Laboratory for Biomedical Research, Ghent University Global Campus, Yeonsu-Gu, Incheon, South Korea
[d] Department of Biochemistry and Microbiology, Universiteit Gent, Ledeganckstraat 35, 9000, Gent, Belgium

ARTICLE INFO

Keywords:
Nanobodies
V_HH
Escherichia coli
Periplasmic expression
Osmotic shock
Purification
Yield

ABSTRACT

Nanobodies are single-domain antibody constructs derived from the variable regions of heavy chain only (V_HH) camelid IgGs. Their small size and single gene format make them amenable to various molecular biology applications that require a protein affinity-based approach. These features, in addition to their high solubility, allows their periplasmic expression, extraction and purification in *E. coli* systems with relative ease, using standardized protocols. However, some Nanobodies are recalcitrant to periplasmic expression, extraction and purification within *E. coli* systems. To improve their expression would require either a change in the expression host, vector or an increased scale of expression, all of which entail an increase in the complexity of their expression, and production cost. However, as shown here, specific changes in the existing standard *E. coli* culture protocol, aimed at reducing breakdown of selective antibiotic pressure, increasing the initial culture inoculum and improving transport to the periplasmic space, rescued the expression of several such refractory Nanobodies. The periplasmic extraction protocol was also changed to ensure efficient osmolysis, prevent both protein degradation and prevent downstream chelation of Ni^{2+} ions during IMAC purification. Adoption of this protocol will lead to an improvement of the expression of Nanobodies in general, and specifically, those that are recalcitrant.

1. Introduction

Nanobodies are small (≈15 kDa) monomeric single-domain antibody constructs derived from the variable regions of either the heavy chain only IgGs derived from camelids (named V_HH) and are similar to heavy chain only immunoglobulin new antigen receptor from nurse sharks (named V_{NAR}) [1–4]. Despite their single domain nature, Nanobodies have been shown to be as specific as conventional monoclonal antibodies, or their derivatives such as single-chain variable fragments (scFvs), and in some cases, even outperforming these [5–7]. Due to their small size and long CDR3 domains, Nanobodies have been shown to engage cryptic epitopes and targets that are not accessible to conventional antibodies [8–13]. Additionally, unlike monoclonal antibodies, Nanobodies have a high thermal stability, resistance to pH and proteases, as well as high solubility [14,15]. As single domain antibody constructs, their simple structure and small size makes them amenable to engineering for various molecular biology applications requiring a protein affinity-based approach [16–19]. Their single gene format as well as non-requirement for post-translational modifications allows their relatively easy periplasmic expression, extraction and purification in using *E. coli* systems using existing standardized protocols adapted from monoclonal or scFv expression [20–22].

Nanobodies are mostly over-expressed in *E. coli* systems [16,23]. As they contain a disulphide linkage between the complementarity determining regions (CDRs) 1 and 3, they require a suitable oxidizing environment to correctly adopt their immunoglobulin fold [20,21,24,25]. This is not possible within the *E. coli* cytoplasm where the presence of thioredoxins contributes to a generally reducing environment [26–30]. Thus, expressed Nanobodies are directed to the *E. coli* periplasmic space. The *E. coli* periplasmic space is the region between the inner plasmalemma and the outer polysaccharide-rich coat of the gram-negative bacteria [31]. This space constitutes a multipurpose compartment which allows for several novel functions, amongst which is protein transport, folding, oxidation and quality control, much akin to the

* Corresponding author. Laboratory of Cellular and Molecular Interactions (CMIM), Vrije Universiteit Brussels, Brussels, Belgium.
E-mail addresses: Christopher.kariuki@vub.be, chriskinya@primateresearch.org (C.K. Kariuki), Stefan.magez@vub.be, Stefan.magez@ghent.ac.kr (S. Magez).

https://doi.org/10.1016/j.pep.2021.105906
Received 19 April 2021; Received in revised form 4 May 2021; Accepted 6 May 2021
Available online 12 May 2021

eukaryotic endoplasmic reticulum [32,33]. The presence of an oxidative environment within the periplasm is the key reason for the directing of the over-expressed Nanobody there. The translocation of the Nanobody, synthesized in the cytoplasm, is achieved post-translationally via an N-terminal peptide signal targeting either the general secretory (Sec) or the twin-arginine-translocation (Tat) pathways [26,34–37]. Of the two, the Sec pathway is the more commonly targeted translocation mechanism applied in our laboratory. To target this pathway, an N-terminal *pelB* leader signal derived from the 22-amino acid leader sequence of pectate lyase B of *Erwinia carotovora* is present on the expression cassette [38]. This signal is cleaved off by a periplasmic signal peptidase after the translocation process, leaving an authentic N-terminus devoid of an N-terminal methionine [38,39].

Periplasmic extraction of Nanobodies is done via osmotic shock [40]. The osmotic shock protocol was first described in experiments involving the extraction of periplasmic enzymes from *E. coli* [41,42]. In this procedure, cells are incubated in a hyperosmotic Tris-buffered sucrose solution containing EDTA. The EDTA permeabilizes their outer membranes by chelation of divalent metal ions required for membrane stability, while the sucrose selectively concentrates in the periplasmic space. The pre-incubated cells are then exposed to a cold hypotonic solution leading to extrusion of the periplasmic contents through the peptidoglycan mesh via osmosis (hence 'osmotic shock') [43]. The periplasmic osmotic shock extraction system offers several advantages when compared to the cytoplasmic extraction of recombinant proteins from *E. coli* cells. Firstly, as previously stated, the periplasmic translocation removes the signal leader thus leaving an authentic N-terminal from the mature protein construct [38,39]. Secondly, the periplasmic extract contains only minimal amounts of cell wall, host derived proteins and cytoplasmic products. Thus, it is anticipated that the purity and yield of an over-expressed recombinant protein within the periplasmic extract obtained should be high.

Some Nanobodies are atypically refractory to *E. coli* periplasmic expression, extraction and purification in the standard protocol. This is in great contrast to the standard expression and purification profiles reported for Nanobodies using this protocol. In situations where there is not sufficient diversity, or where the Nanobodies in question are of high value (e.g., with good binding affinities), then it becomes imperative to improve their expression, extraction and purification. Amongst the choices for improving the expression are either a change in the expression host, vector, or an increased scale of expression, all of which entail an increase in the complexity of their expression, not to mention the additional cost. In this study, the expression of several refractory Nanobodies was improved by simple modifications to the existing standard culture and extraction protocol.

2. Methods

2.1. Nanobody sequence analysis

The plasmids (Fig. 1B; Supplementary Appendix 3 Fig. 1) with inserts encoding the different V_HH gene sequences were obtained by growing out *E. coli* WK6 glycerol stocks from the CMIM laboratory at the VUB, Belgium. After an overnight pre-culture, plasmids were extracted from the cells using the GenElute™ Plasmid Miniprep Kit (Sigma Aldrich). PCR was carried out using plasmid-based primers (pHEN6C – M13F and M13R) to confirm insertion. Sanger sequencing was subsequently carried out on the extracted plasmids using the same primer sets for each plasmid.

Selected colonies showing correctly sized V_HH inserts in the proper orientation and translating into an open reading frame encoding V_HH/Nanobody protein as simulated by CLC Main WorkBench (Qiagen) were approved for production. Glycerol stocks were prepared by adding 500 μL of 50% glycerol to 500 μL of overnight culture in LB supplemented with 100 μg mL^{-1} ampicillin and 0.1% glucose. These were stored at −80 °C for future production of Nanobodies.

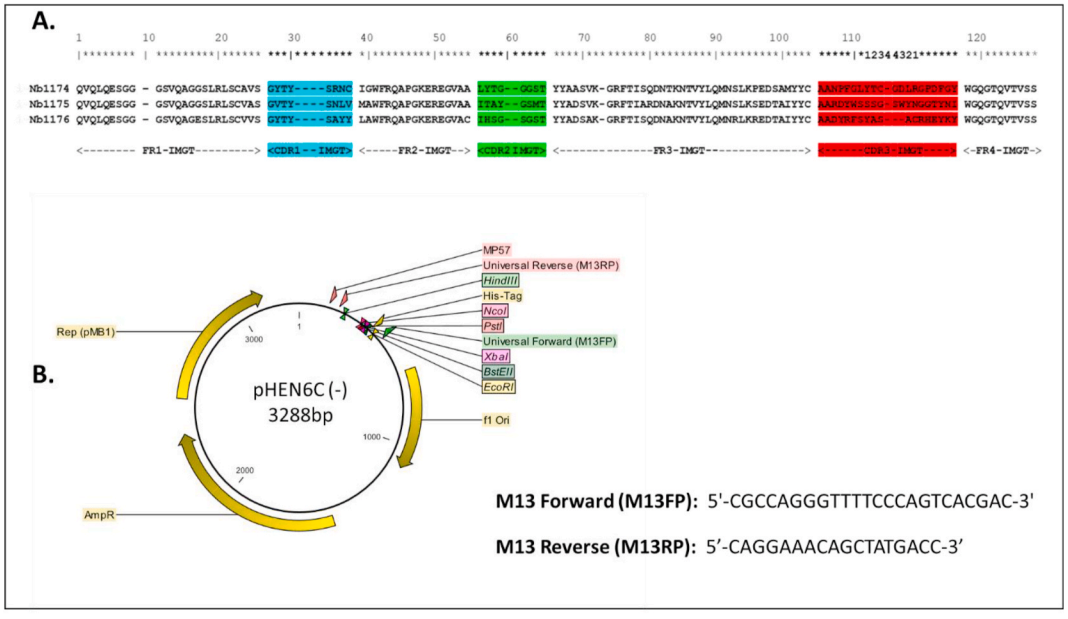

Fig. 1. (A) IMGT alignment of select translated cDNA from Sanger sequencing of Nanobody gene insertions within the pHEN6C plasmid using primer M13RP and M13FP: The IMGT numbering system for variable regions of immunoglobulins relies on the high conservation of the structure of the variable region and denotes framework regions as FR and complementarity determining regions as CDR. Thus, FR1 - IMGT refers to position 1–26, FR2 - IMGT to 39–55, FR3 - IMGT to 66–104 and FR4-IMGT to 118 – 128. Accordingly, CDR1 – IMGT refers to position 27 – 38, CDR2 – IMGT to 56 – 65 and CDR3 – IMGT to position 105 – 117. To maintain the positions, in light of CDR variability, gaps are introduced within the CDRs as utilized in 2-D graphical representations (designated as IMGT Colliers de Perles) [48,49] and in 3D structures in the IMGT/3D structure [50]. Thus, in a sequence alignment, gaps in the CDR1-IMGT (less than 12 residues long) and the CDR2-IMGT (less than 10 residues long) are put from the 'top' of the CDR-IMGT loops. Gaps in the CDR3-IMGT (basic length of 13 residues) are introduced in the same way when there are less than 13 residues. When there are more than 13 residues, additional positions are introduced between position 111 and 112 and labelled with whole numbers as seen in the alignment at A above. (B) The pHEN6C plasmid map indicating the positions of the M13RP and M13FP primers.

2.2. ExPASy analysis

Using the derived, and confirmed V_HH gene sequences, open reading frames were then characterized *in silico* using the online ProtParam tool, ExPASy: (https://web.expasy.org/protparam/).

Molecular weight, pI, instability index and the extinction coefficient were calculated, based on the Nanobody sequences.

2.3. Production and extraction using standard expression protocol

Standard expression of the Nanobodies was carried out using the protocol as previously described [44]. A detailed protocol can be found in Appendix 1 in the Supplementary information.

Briefly, pre-cultures (per Nanobody) were prepared by inoculation from glycerol stocks into LB media (10 mL max per 50 mL sterile conical bottomed tubes (BD Biosciences)) supplemented with a final concentration of 100 μg mL^{-1} ampicillin (Duchefa Biochemie), 2 mM $MgCl_2$ (Sigma Aldrich) and 0.1% glucose (Duchefa Biochemie). These pre-cultures (approximately 2 tubes per Nanobody) were incubated overnight at 37 °C with aeration (200 rpm).

The main culture (5 L per Nanobody) was started by inoculating 15 baffled flasks (each with a capacity of 1 L) each containing 330 mL of TB medium supplemented with a final concentration of 100 μg mL^{-1} ampicillin, 0.1% glucose and 2 mM $MgCl_2$ with a 330-fold dilution of the pre-culture i.e., 1 mL pre-culture per 330 mL of TB media. The culture was then incubated at 37 °C with aeration (200 rpm max) until an optical density at 600 nm (OD_{600}) = 0.6–0.8 was achieved. The incubation temperature was then lowered to 28 °C.

Nanobody expression was induced by addition of 1 mM IPTG (Duchefa Biochemie) followed by incubation with aeration (200 rpm max) for ≥ 16 h. Cells were pelleted by centrifugation (11,305 g, 10 min, at 14 °C) and the periplasmic proteins extracted by osmotic shock via addition of ice-cold TES buffer (4 mL TES/330 mL of culture) for 6 h while shaking, followed by addition of ice-cold TES/4 buffer (8 mL TES/4 for 330 mL of culture) and overnight incubation on ice while shaking at 200 rpm and 4 °C. To saturate the EDTA within the TES buffer, 2 mM $MgCl_2$ (Sigma Aldrich) was added to the suspension (300 μL 2 M $MgCl_2$ for 330 mL of culture). The periplasmic extract (supernatant) was harvested by centrifugation (11,305 g; 30 min, at 4 °C) and kept aside for purification. The extraction protocol was then repeated on the resuspended cell pellets for a second time, but with reduced TES (2 h) and TES/4 (4 h) incubation times.

2.4. Production and extraction using modified expression protocol

In a bid to achieve an increased Nanobody yield production, a modified protocol was run. In this protocol, several factors i.e., culture media, pre-culture temperature, culture time, culture temperature and extraction methods, were changed (Table 1& Appendix 2). The glycerol stocks used remained the same.

Table 1
Comparison between the standard and modified expression protocols for Nanobody® production.

	Standard Protocol	Modified Protocol
Media used	Terrific Broth	2xTY
Pre-culture temperature	37 °C	30 °C
Pre-culture/Culture ratio	1:300	1:30
IPTG concentration used	1 mM	0.25 mM
Culture temperature after induction	28 °C	37 °C
Culture time after induction	>14 h	Max 4 h
Osmotic shock after TES	TES/4 (4-fold diluted TES)	5 mM $MgSO_4$
IMAC column volume (per liter of culture)	1 mL	0.5 mL

Briefly, pre-cultures (per Nanobody) were prepared by inoculation from the glycerol stock into 150 mL 2xTY supplemented with a final concentration of 100 μg mL^{-1} ampicillin, 2 mM $MgCl_2$ and 0.5% glucose. These pre-cultures were incubated overnight at 30 °C with aeration (200 rpm). The pre-cultures were harvested by centrifuging (3000 g, 10 min, at 20 °C) in sterile 50 mL conical bottomed tubes (BD Biosciences), and the supernatant discarded. The pellet was then resuspended in 30 mL 2xTY media supplemented with 100 μg mL^{-1} ampicillin and 0.5% glucose.

The main culture (5 L per Nanobody) was started by inoculating 15 baffled flasks (each with a capacity of 1 L) each containing 330 mL of 2xTY medium supplemented with a final concentration of 100 μg mL^{-1} ampicillin, 0.5% glucose and 2 mM $MgCl_2$ with 2 mL of the dissolved pre-culture pellet. The culture was then incubated at 37 °C with aeration (220 rpm max) until an optical density at 600 nm (OD_{600}) = 0.6–0.8 was achieved.

Nanobody expression was then induced at the same temperature (37 °C) by addition of 0.25 mM IPTG followed by incubation with aeration (220 rpm max) for 4 h. Cells were pelleted by centrifugation (11,305 g, 10 min, at 14 °C) and the periplasmic proteins extracted by osmotic shock via addition of ice-cold TES buffer (4 mL TES/330 mL of culture) overnight hours while shaking at 200 rpm and 4 °C. Lysozyme (0.5–1 mg per liter of bacterial culture) and DNAse (10 μg per liter of bacterial culture) were supplemented in the TES. The following day, osmotic shock was applied by addition of ice-cold 5 mM $MgSO_4$ (8 mL per 330 mL of culture) for 2 h. The periplasmic extract (supernatant) was harvested by centrifugation (11,305 g; 30 min, 4 °C) and kept aside for purification. The extraction protocol was then repeated on the resuspended cell pellets for a second time, but with reduced TES (1 h) and ice-cold 5 mM $MgCl_2$ (2 h) incubation times.

2.5. Purification of extracted Nanobodies

A HIS-select nickel affinity gel (Sigma Aldrich) was prepared by washing 2X with Milli-Q H_2O by centrifugation at 353*g* for 7 min at 20 °C. A third wash with phosphate binding buffer {22 mM $NaH_2PO_4{\cdot}H_2O$ & 77 mM anhydrous Na_2HPO_4, 500 mM NaCl (pH 7.4)} or PBS containing 500 mM NaCl, was carried out at the same centrifugation conditions. The HIS-select nickel affinity gel was then incubated with the periplasmic extract at room temperature for 1 h with gentle shaking.

In the meantime, a PD-10 column was prepared, and the column loaded with 5 mL of phosphate binding buffer to ensure free flow of buffer through the filter. The column was packed with the loaded HIS-select nickel affinity gel beads and drained by gravity. The unbound proteins were washed off the gel matrix with 20 column volumes of phosphate binding buffer.

The bound His-tagged Nanobodies were eluted with stepwise addition of 1 mL 1 M imidazole buffer (to a total amount of 5 mL per 1 mL of His-Select nickel affinity gel beads) in PBS containing 500 mM NaCl and 1 M imidazole (Sigma Aldrich) (pH 7.5). Aliquots were obtained from the fractions, then processed for SDS-PAGE and western blot analysis. The protein concentrations were estimated by measuring the absorbance at 280 nm (A_{280}) on a NanoDrop ND-1000 spectrophotometer (Isogene) and applying the extinction coefficient. Fractions containing the Nanobody of interest as visualized by SDS-PAGE were pooled and kept aside for further purification.

The affinity purified histidine tagged Nanobodies were further purified by size exclusion gel filtration to separate out any remaining co-purifying contaminants. For the gel filtration, a Superdex 75 (S75) 10 mm/300 mm (=~24 mL) or 16 mm/60 cm (=~120 mL) column (GE Healthcare) was pre-equilibrated with at least one column volume of phosphate buffered Saline (PBS) buffer {with 500 mM NaCl (pH 7.4)} on an Akta Explorer platform (GE Healthcare) or a BioRad NGC (BioRad). Aliquots were obtained from peak fractions, then processed for SDS-PAGE and western blot analysis. Fractions containing the Nanobody of interest were pooled, and absorbance at 280 nm (Abs_{280}) measured with

a NanoDrop ND-1000 spectrophotometer (Isogene). The protein concentration was then estimated using their extinction coefficient. These were then concentrated using Vivaspin protein concentrator columns with a 5000 Da MW Cut-Off (Sartorius) and stored at 4 °C.

2.6. Quality control of expressed nanobodies using SDS-PAGE, western blotting and thermoflour analysis

2.6.1. SDS-PAGE analysis

Aliquots taken at different steps of the expression and purification protocol were subjected to SDS-PAGE analysis [45]to visualize the expression profile as well as the purification progress. Aliquots of 1 mL of the bacterial cultures taken from pre-cultures, before induction, and after overnight incubation of the induced culture were used. The samples were centrifuged for 3 min at maximum RPM and pellets re-suspended in 45 μL of water (filtered and sterilized). These were then boiled for 5 min at > 90 °C and subsequently stored at 4 °C. Prior to loading on SDS- PAGE, the samples were normalized to an OD_{600} of 0.25 by appropriate dilution in Milli-Q water (filtered and sterilized), then boiled a second time at > 90 °C for 10 min with 25 μL of NuPage LDS sample buffer (4 X, supplemented with 50 mM DTT) in a total SDS-PAGE sample volume of 100 μL. All samples for SDS-PAGE analysis were loaded in duplicate at max 30 μL per well on a 10% acrylamide gel (BioRad Criterion XT 10% Bis-Tris precast gel). Gel electrophoresis was performed in 1 X MES buffer at 150 V until sufficient migration had occurred. Protein bands were visualized by staining with Coomassie Brilliant Blue R250 and molecular masses determined by estimation in comparison to the PageRuler Prestained Protein Molecular Weight Marker (ThermoFisher).

2.6.2. Western blotting

Western blotting was performed as described previously [46]. Briefly, the proteins were transferred from the electrophoresed polyacrylamide gel to either methanol - activated PVDF (ThermoFisher) or nitrocellulose with 0.45 μm pores (Amersham) membranes using a Bio-Rad wet transfer system with a tris-glycine buffer supplemented with methanol. The transfer process was carried out at 100 V for 1 h at room temperature with cooling provided by using a cooling cassette (previously stored at −80 °C) inserted in the wet transfer system and a magnetic stirring bar for circulation.

The membranes were blocked overnight at 4 °C in 5% BSA in PBS with shaking and subsequently washed 3 times with PBS-Tween 20 (0.1%). For detection of the Nanobodies, 2.5 μL of the primary antibody (biotinylated mouse anti-His (ThermoFisher)) in 20 mL of 5% BSA in PBS was added to the membrane with an incubation of 1 h at room temperature. The membrane was then washed 3 times with PBS-Tween 20 (0.1%), with 5 min per wash before being incubated for 1 h with 2.5 μL of the secondary ligand (Streptavidin conjugated with Horseradish peroxidase (ThermoFisher)) in 20 mL of 5% BSA in PBS. After the incubation, the membrane was again washed 3 times with PBS-Tween 20 (0.1%), with 5 min per wash. The blot was developed chromogenically with the Pierce CN/DAB substrate kit (ThermoFisher).

2.6.3. Differential scanning fluorimetry

The thermostability of select monovalent Nanobodies was measured by differential scanning fluorimetry (Thermofluor) on a real-time PCR machine (Applied Biosystems 7500), in a 96-well plate format with a final volume of 25 μL in each well. For the buffer blank, 2 μL of 25 X SYPRO orange dye (Life Technologies) was mixed with 23 μL of PBS buffer (containing 500 mM NaCl (pH 7.4)). For the Nanobody® samples, 2 μL of 25X SYPRO orange dye (Life Technologies) was mixed with 25 μL of the Nanobody® of interest at a final concentration of at least 0.4 mg mL^{-1} in PBS buffer containing 500 mM NaCl (pH 7.4)). Data for all samples were collected in triplicate. The fluorescence was measured with increasing temperature, starting at 5 °C, and increasing the temperature by 0.5 °C per minute up to 95 °C. To obtain buffer-corrected fluorescence signals for each Nanobody, the averaged buffer data set was subtracted from the averaged protein data set. The buffer-corrected fluorescence signal (F) was plotted as a function of temperature (T) and fitted with the Boltzmann sigmoidal function to obtain the melting temperature (T_m) using the equation

$$F = F_0 + \frac{F_{max} - F_0}{1 + e^{\frac{T_m - T}{a}}}$$

Where F_0 and F_{max} are the lowest (pre-transitional) and the highest (post-transitional) buffer corrected fluorescence signals (expressed in AU) and α is the change in T corresponding to the most significant change in F (also called the slope of the transition region, expressed in AU/°C) [47].

3. Results

In total, 6 Nanobodies were expressed using the modified protocol (Table 1). Three of them, Nb 1174, 1175 and 1176 were expressed with both standard and modified protocol in a comparative manner. The other three, Nb SH-75, Nb 60 and Nb 2RS15d were expressed with only the modified protocol, with the previous yields from the standard expression protocol indicated as reported.

The Sanger - sequenced and translated cDNA sequences of three selected monovalent Nanobodies (Nbs) indicated that they were inserted in the correct orientation and open reading frame within their expression pHEN6C plasmid (Fig. 1A and B).

Additionally, the three Nbs were confirmed to have the V_HH hallmark amino acid substitutions in framework 2 (V37F, G44E, L45R and W47X) in accordance to Kabat/IMGT numbering (Fig. 1A.) [51,52]. The three Nanobody cDNA sequences also displayed the characteristic cysteine residues at positions 22 and 106 necessary for formation of a disulfide bridge between the Framework 1 and Framework 3 regions [4, 53].

Global protein parameters for the Nanobodies were derived *in silico* using the Protparam tool [54] from Expasy resource portal (Table 2)..

The six monovalent Nanobodies were then over-expressed in *E. coli* WK6 cells. The over-expression of the comparatively prepared three (1174, 1175 & 1176) using the standard operating protocol in comparison to the modified expression protocol did not appear to have significant differences as judged by the polyacrylamide gel profiles generated. (Fig. 2A.&B). In western blot though, the over-expression of the test Nanobodies (Nb 60, Nb SH-75 & Nb 2Rs15d) can be seen increasing over the sampling period (Supplementary Appendix 3 Fig. 2). However, upon purification after extraction via osmotic shock, there were changes observed in the gel profile between the two protocols for the comparatively run three Nanobodies (1174, 1175 & 1176). In particular, the second elution step (Elution 2) of the IMAC from the modified protocol appeared to have much more contaminants than of the similar step in the standard protocol.

After IMAC, size exclusion chromatography is typically used as a secondary purification step for purification of Nanobodies. At this point, all the monovalent Nanobodies, when expressed with the standard protocol, could not be purified using the preparative large-scale SEC as their yields were too low. This meant that to achieve the polishing step, a smaller SEC column (S75 10 mm/300 mm (=~24 mL)) was used (Fig. 3A.). This translated to a lower final yield of pure Nanobodies. In comparison, the same Nanobodies, when produced via the modified protocol, gave higher yield, therefore meaning that to achieve the size exclusion purification step, a larger scale of preparative column (16 mm/60 cm (=~120 mL)) could be utilized (Fig. 3B.).

To measure the yields comparatively, the pure protein yield (in milligrams) per liter of culture used was calculated (Table 3). It was observed that there was at least a 3-fold increase in the yield of two of the comparatively prepared refractory Nanobodies (Nb 1174 and 1176). In one of the test cases, Nb_60, there was a 9-fold increase in the expression.

Table 2
Nanobodies properties as estimated using the Protparam tool (https://web.expasy.org/protparam/) from the Expasy resource portal.*Test cases that were previously shown to be refractory, kindly provided by internal collaborators, see Acknowledgements.

Protein	Vector	No of residues	pI	Molecular Weight (kDa)	Extinction coefficient	Abs 0.1% (1 g/L)
Nb_ 1174	**pHEN6c**	134	7.9	14.5	26150	1.81
Nb_ 1175	**pHEN6c**	134	8.6	14.6	37025	2.53
Nb_ 1176	**pHEN6c**	132	8.4	14.8	30620	2.067
***Nb_ 60**	**pHEN6c**	146	5.0	15.9	41620	2.60
***Nb_ SH75**	**pMECs**	143	6.7	15.54	37610	2.42
***Nb_2Rs15d-myc**	**pHEN25**	136	7.3	14.89	25690	1.73

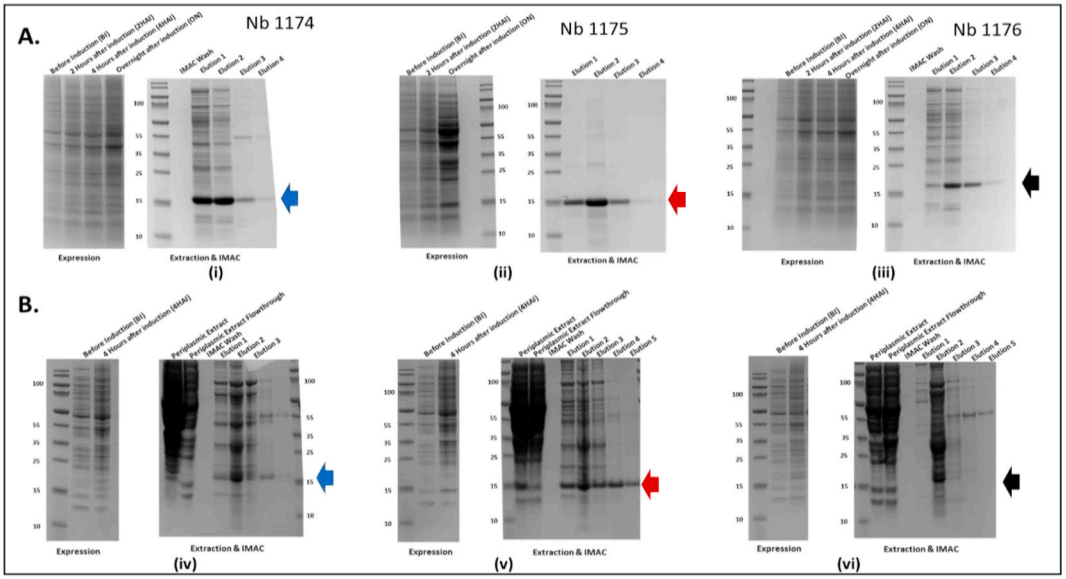

Fig. 2. Expression and IMAC purification Coomassie-stained polyacrylamide gel profiles for over-expressed Nanobodies 1174, 1175 & 1176. Panel A gives the profiles for over-expression with the standard protocol, while panel B gives the profiles for over-expression with the modified protocol.

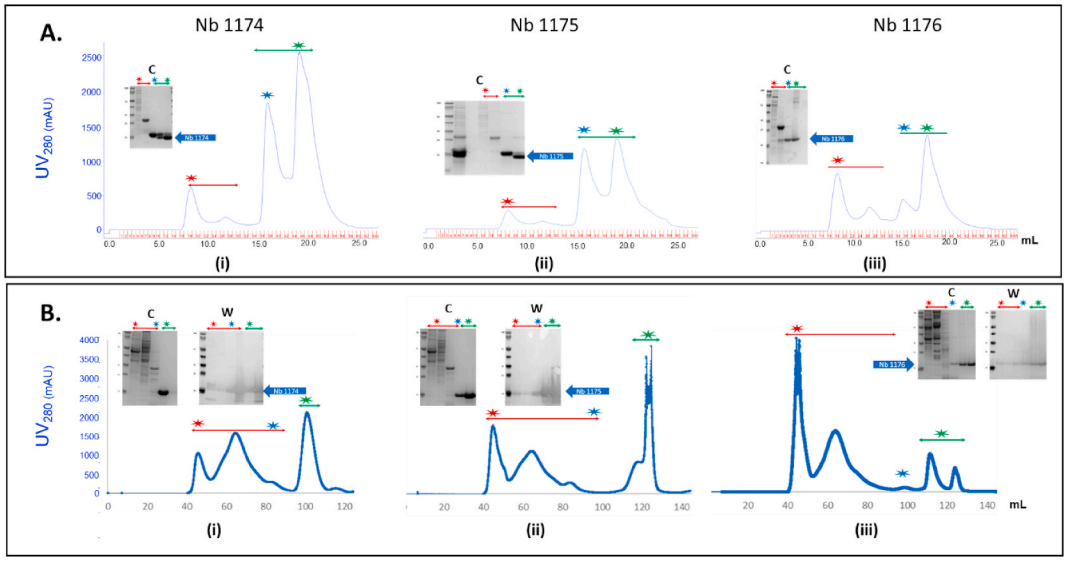

Fig. 3. Size exclusion chromatography of IMAC purified Nanobodies 1174, 1175 & 1176. Panel A indicates the purification of Nanobodies from standard expression protocol, while B indicates purification from the modified expression protocol. Inset within each curve, are the polyacrylamide gel (C) and western blot (W) profile for each purified Nanobody. Here a difference in yield is observed, as the panel A represents the curves from the smaller SEC column (S75 10 mm/300 mm (=~24 mL)) thus giving lower yields, while panel B represents the curves from the larger preparative SEC column (S75 16 mm/60 cm (=~120 mL)) thus giving higher yields.

Table 3
Nanobodies have an increased yield per liter of culture after the modification of the expression SOP. Nanobodies that were refractory to expression had at least a threefold increase in extracted and purified protein. *(The yield of the non-refractory Nanobody y. i.e., Nb 1175 did not change).#(These Nanobodies were expressed as test cases for the modified protocol. Further information on their vectors and purification is provided in the supplementary).

Protein	Vector	Yield (mg/liter of culture) after Standard SOP	Yield (mg/liter of culture) after modified SOP	Fold increase
Nb_ 1174	**pHEN6c**	0.7	**4.3**	6
Nb_ 1175	**pHEN6c**	5	**5.6**	1*
Nb_ 1176	**pHEN6c**	0.5	**1.4**	3
#Nb_ 60	**pHEN6c**	0.25	**2.21**	9
#Nb_ SH75	**pMECs**	0.6	**1.14**	2
#Nb_2Rs15d-myc	**pHEN25**	2	**4.49**	2

Differential scanning fluorimetry of the Nanobodies did not reveal significant changes in the melting temperatures (Fig. 4 A &B).

4. Discussion

Nanobodies are recombinantly produced small antigen binding domains derived from the variable regions (V_HHs) of camelid heavy-chain only antibodies (H_{cab}) [55,56]. They are mostly expressed in the prokaryotic expression host, *E. coli*, using well-established standard operating protocols [16,23,44].

Due to their requirement for proper disulphide linkage between their CDR1 and CDR3, folding of Nanobodies occurs primarily within the *E. coli* periplasmic space [20,25]. However, their transcription and translation occurs within the cytoplasm. Therefore, the folding protein needs to be translocated post-translationally to the periplasmic space via the general secretory pathway i.e., the Sec translocon [35]. Post-translational translocation to the periplasm is made possible via the hydrophobic *pelB* secretion signal on the N-terminus of the construct [38]. Once the nascent protein emerges from the ribosome, it binds to the trigger factor, followed by the binding of Sec B then Sec A [36,57]. This complex of SecA bound preproteins is then bound by the SecYEG translocase, which initiates the translocation process [35,36,57]. Thus, prior to translocation, preproteins must be maintained in an export competent conformation in the cytoplasm, which is thought to be a protease sensitive, loosely folded structure [35,36,39,57].

Variable antibody (V_{ab}) fragments have been successfully expressed in *E. coli* using induction at high temperatures [58]. However, the standard Nanobody protocol is designed for IPTG induced protein expression at 28 °C [23,44]. While this enhances the expression of the proteins, and minimizes proteolytic degradation, efficient translocation to the correct folding environment can be hindered at this low temperature. This is exacerbated when the recombinant protein is very efficiently expressed by an induction step, quickly overwhelming the cell's capacity to maintain the protein in an unfolded export competent state before periplasmic translocation. This subsequently leads to an accumulation of expressed protein in the cytoplasm, mostly in a translocation-incompetent state, with the concomitant poor periplasmic yields. Previous work in our laboratory has established that the poor yield of such refractory Nanobodies can be resolved partially by freeze thawing the derived cell pellets, yielding dramatically higher amounts of proteins. Thus, poor yield exhibited by these Nanobodies can be attributed to the failure to translocate from the cytoplasm leading to their poor periplasmic extraction and purification profiles. However, as the freeze-thaw methods entails cell breakage, there are concerns about the folding state of the Nanobodies, proteolytic damage, as well as the presence of the un-cleaved signal peptide. We hypothesized that providing a higher expression temperature i.e., 37 °C would lead to improved periplasmic translocation and therefore better extraction and purification profiles. Due to the chance of increased degradative proteolytic activity at 37 °C within the periplasm, in addition to heightened breakdown of the selective antibiotic pressure, we empirically optimized the expression time down from the normal overnight expression (>16 h) to 4 h.

The Nanobody starting stock (preculture) of *E. coli* containing our recombinant Nanobody gene was grown atypically, at a low temperature (25–30 °C) and in a large volume for an eventual low pre-culture-to-culture volume ratio (1:30). In contrast, the typical Nanobody preculture is grown at 37 °C and with an eventual high pre-culture-to-culture volume ratio (1:300). The reason for this change was two-fold. Firstly, the secretion of beta-lactamase, the enzyme responsible for antibiotic selectivity, was reduced at these low temperatures. The enzyme is translocated co-translationally by the Sec translocon from the cytoplasm to the periplasm. Therefore, using the standard pre-culture

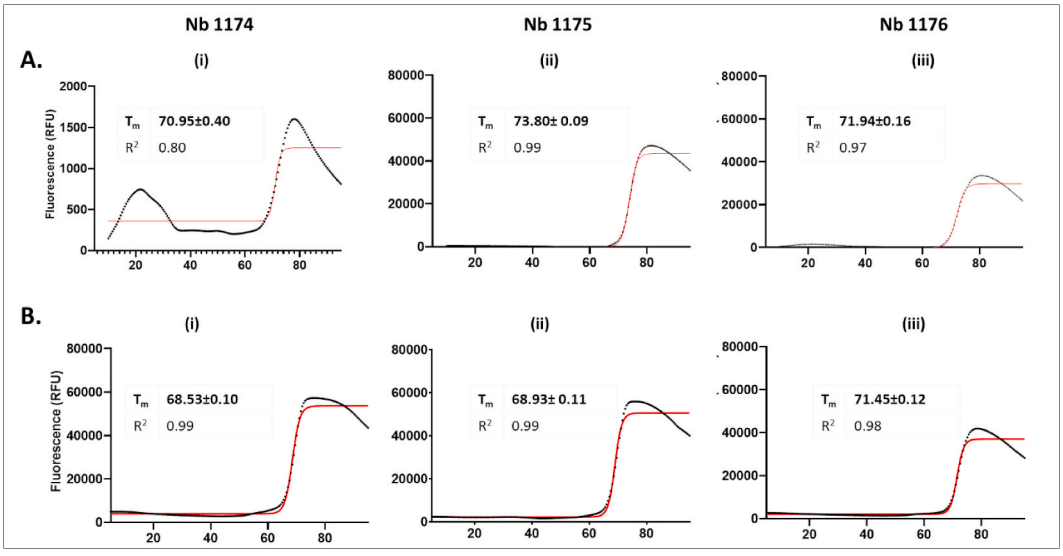

Fig. 4. Graphs illustrating the thermal shift assay (Thermofluor) results for select monovalent Nanobodies before and after using the modified expression and extraction SOP. Results do not indicate a significant change in the melting temperature (T_m), thus showing that the protein proteins' thermal properties are not changed by using the modified SOP. Measurements were done in triplicate and corrected for the buffer baseline, leading to the data points shown in black. A non-linear Boltzmann-Sigmoidal curve is fitted onto the data (red line). The T_m is calculated as the temperature where half of the hydrophobic residues are exposed.

temperature of 37 °C, the enzyme is efficiently translocated to the periplasm for maturation and secretion. This means that, over the course of a typical overnight pre-culture, the selective antibiotic pressure applied on the cells greatly diminishes. Further after the overnight incubation, the pre-culture is typically diluted to a 1:300 preculture-to-culture volume ratio. However, the enzyme secreted over the overnight incubation is also transferred to the new sub-culture thereby already diminishing selective pressure from the antibiotic used. We resolved the enzyme carry-over problem as mentioned above, by growing a large volume of the pre-culture, then centrifuging it to remove the enzyme containing supernatant. It was necessary to grow large pre-culture volume overnight, to achieve enough cells for the main culture. The pellet from the pre-culture centrifugation step was then resuspended in a smaller volume of culture medium before inoculation. This ensured a low ratio of pre-culture to culture and limited transfer of the overnight secreted beta-lactamase to the main culture.

Extraction of the expressed Nanobodies within the periplasm is achieved by osmotic shock [23,44]. The osmotic shock is achieved by initially pre-incubating cells with a hyperosmotic Tris-EDTA-sucrose (TES) buffer. To achieve maximum release of proteins from the periplasm, the osmotic shock requires cold conditions [41,42,59]. Under typical circumstances, this is then followed by addition of a cold four-fold diluted TES solution (TES/4). In this study, we found that the use of a dilute and ice-cold solution of magnesium sulfate (5 mM $MgSO_4$), achieved the same effect as the TES/4. We postulated that the use of $MgSO_4$ to extract the Nanobodies via osmotic shock would serve the purpose of complexing the EDTA within the TES, therefore avoiding chelation of the Ni^{2+} ions during the subsequent IMAC. In line with literature, we also used lysozyme and DNAse during the osmotic shock to enhance the periplasmic yield of the refractory Nanobodies [41,42]. However, we do not deem the addition of lysozyme to be necessary, for two reasons. The first is that for a reduction in costs and complexity, the procedure must be as simple as possible in comparison to the original protocol. Secondly, if the Nanobodies are over-expressed and present in the periplasm in adequately high concentrations, then gentle resuspension of the cells by shaking during the osmotic shock is adequate for their release from the periplasm. The resuspension of cells by gentle agitation is necessary to avoid the breakage of the spheroblasts, leading to chromosomal DNA contamination of the periplasmic extract. This then leads to a fouling during the downstream IMAC chromatography. Thus, after a gentle resuspension, the addition of DNAse is also not considered necessary. The exception is of course, when there is an unprecedented amount of cell lysis, usually presenting as a slurry pellet after osmotic shock and centrifugation.

Enhancement of the IMAC purification of the Nanobodies was also adopted in the improved protocol. This was done by reducing the IMAC column size to 0.5 mL of Ni-NTA slurry instead of 1 mL per liter of culture. This increased the specific attachment of the C-terminal Nanobody hexa-histidine tag, instead of the bacterial contaminants with histidine stretches, due to their competitive affinity for the Ni^{2+} ions. As can be observed in the gel images presented, this resulted in a relatively pure protein with a prominent band at the expected size (about 15 kDa). Further improvements proposed for adoption to the modified protocol include adding imidazole (up to 20 mM) in the washing buffer to remove the high molecular weight bacterial contaminants observed in the IMAC elution and appearing early in SEC profile.

Thermal shift analyses (TSA) using differential scanning fluorimetry (DSF) indicate that the extracted Nanobodies retained their characteristics, giving similar thermal melt profiles as those derived using the standard procedures. This further enhanced our confidence that the procedures we applied did not result in a drastic change in the expressed product, despite there being a favorable change in yield.

5. Conclusion

Here, we demonstrate the yield enhancement from Nanobodies extracted from the periplasm by taking into consideration the biology of the expression host *E. coli*. Utilizing the temperature at which the *E. coli* Sec translocon operates most efficiently, we were able to reduce both the destruction of the selective antibiotic agent as well as enhance the periplasmic translocation of expressed Nanobodies. Using legacy extraction procedures derived from literature, into the standard production protocol, allowed us to enhance the extraction and purification of the expressed Nanobodies by several fold. We therefore propose this modified protocol as a substitute for the expression of refractory Nanobodies.

Disclosure

CK conceived and developed the modified protocol and performed the experimental work detailed in the manuscript. All authors contributed equally to the development of the manuscript.

Funding

The authors acknowledge the financial support of the Interuniversity Attraction Pole Program (PAI-IAP N. P7/41, http://www.belspo.be/belspo/iap/index_en.stm). CK is a PhD research fellow and graduate teaching assistant under the Vrije Universiteit Brussels Faculty of Science (WE) under the AAP mandate.

Declaration of competing interest

None.

Acknowledgements

The authors gratefully acknowledge the kind gifts of the pMECs-Nb SH 75 (Drs Ema Romao and Prof. Dr. Serge Muyldermans), the pHEN25-2Rs15d-myc (Jan de Jonge and Prof. Dr. Nick Devoogdt) and the pHEN6c-Nb 60 (Andrès Alvarez Rodriguez and Dr. Joar Pinto).

Appendix A. Supplementary data

Supplementary data to this article can be found online at https://doi.org/10.1016/j.pep.2021.105906.

References

[1] V. Nguyen, C. Su, S. Muyldermans, W. Van Der Loo, Heavy-chain antibodies in *Camelidae*; a case of evolutionary innovation, Immunogenetics 54 (2002) 39–47, https://doi.org/10.1007/s00251-002-0433-0.
[2] H. Dooley, M.F. Flajnik, Antibody repertoire development in cartilaginous fish, Dev. Comp. Immunol. 30 (2006) 43–56, https://doi.org/10.1016/j.dci.2005.06.022.
[3] D. Könning, S. Zielonka, J. Grzeschik, M. Empting, B. Valldorf, S. Krah, C. Schröter, C. Sellmann, B. Hock, H. Kolmar, Camelid and shark single domain antibodies: structural features and therapeutic potential, Curr. Opin. Struct. Biol. 45 (2017) 10–16, https://doi.org/10.1016/j.sbi.2016.10.019.
[4] C. Hamers-Casterman, T. Atarhouch, S. Muyldermans, G. Robinson, C. Hamers, E. B. Songa, N. Bendahman, R. Hamers, Naturally occurring antibodies devoid of light chains, Nature 363 (1993) 446–448, https://doi.org/10.1038/363446a0.
[5] A.H. Laustsen, J. María Gutiérrez, C. Knudsen, K.H. Johansen, E. Bermúdez-Méndez, F.A. Cerni, J.A. Jürgensen, L. Ledsgaard, A. Martos-Esteban, M. Øhlenschlæger, U. Pus, M.R. Andersen, B. Lomonte, M. Engmark, M.B. Pucca, Pros and cons of different therapeutic antibody formats for recombinant antivenom development, Toxicon 146 (2018) 151–175, https://doi.org/10.1016/j.toxicon.2018.03.004.
[6] S. Muyldermans, Single domain camel antibodies: current status, Rev. Mol. Biotechnol. 74 (2001) 277–302, https://doi.org/10.1016/S1389-0352(01)00021-6.
[7] A. Desmyter, S. Spinelli, A. Roussel, C. Cambillau, Camelid nanobodies: killing two birds with one stone, Curr. Opin. Struct. Biol. 32 (2015) 1–8, https://doi.org/10.1016/j.sbi.2015.01.001.
[8] K.E. Conrath, M. Lauwereys, M. Galleni, A. Matagne, J.-M. Frere, J. Kinne, L. Wyns, S. Muyldermans, Beta-lactamase inhibitors derived from single-domain antibody fragments elicited in the *Camelidae*, Antimicrob. Agents Chemother. 45 (2001) 2807–2812, https://doi.org/10.1128/AAC.45.10.2807–2812.2001.

[9] T.N. Baral, S. Magez, B. Stijlemans, K. Conrath, B. Vanhollebeke, E. Pays, S. Muyldermans, P. De Baetselier, Experimental therapy of African trypanosomiasis with a Nanobody-conjugated human trypanolytic factor, Nat. Med. 12 (2006) 580–584, https://doi.org/10.1038/nm1395.
[10] B. Stijlemans, K. Conrath, V. Cortez-Retamozo, H. Van Xong, L. Wyns, P. Senter, H. Revets, P. De Baetselier, S. Muyldermans, S. Magez, Efficient targeting of conserved cryptic epitopes of infectious agents by single domain antibodies: african trypanosomes as paradigm, J. Biol. Chem. 279 (2004) 1256–1261, https://doi.org/10.1074/jbc.M307341200.
[11] S.B. Ditlev, R. Florea, M. a Nielsen, T.G. Theander, S. Magez, P. Boeuf, A. Salanti, Utilizing Nanobody technology to target non-immunodominant domains of VAR2CSA, PloS One 9 (2014), e84981, https://doi.org/10.1371/journal.pone.0084981.
[12] M. Lauwereys, M. Arbabi Ghahroudi, A. Desmyter, J. Kinne, W. Holzer, E. De Genst, L. Wyns, S. Muyldermans, Potent enzyme inhibitors derived from dromedary, Eur. Mol. Biol. Organ. J. 17 (1998) 3512–3520, https://doi.org/10.1093/emboj/17.13.3512.
[13] E. De Genst, K. Silence, K. Decanniere, K. Conrath, R. Loris, J. Kinne, S. Muyldermans, L. Wyns, E. De Genst, K. Silence, K. Decanniere, K. Conrath, R. Loris, J. Kinne, S. Muyldermans, L. Wyns, Molecular basis for the preferential cleft recognition by dromedary heavy-chain antibodies, Proc. Natl. Acad. Sci. U. S. A. 103 (2006) 4586–4591, https://doi.org/10.1073/pnas.0505379103.
[14] N. Goris, F. Vandenbussche, K. De Clercq, Potential of antiviral therapy and prophylaxis for controlling RNA viral infections of livestock, Antivir. Res. 78 (2008) 170–178, https://doi.org/10.1007/s00253-007-1142-2.
[15] R.H.J. Van Der Linden, L.G.J. Frenken, B. De Geus, M.M. Harmsen, R.C. Ruuls, W. Stok, L. De Ron, S. Wilson, P. Davis, C.T. Verrips, Comparison of physical chemical properties of llama V(HH) antibody fragments and mouse monoclonal antibodies, Biochim. Biophys. Acta Protein Struct. Mol. Enzymol. 1431 (1999) 37–46, https://doi.org/10.1016/S0167-4838(99)00030-8.
[16] E. Romao, F. Morales-Yanez, Y. Hu, M. Crauwels, P. Pauw, G. Hassanzadeh, N. Devoogdt, C. Ackaert, C. Vincke, S. Muyldermans, Identification of useful Nanobodies by phage display of immune single domain libraries derived from camelid heavy chain antibodies, Curr. Pharmaceut. Des. 22 (2016) 6500–6518, https://doi.org/10.2174/1381612822666160923114417.
[17] Y. Hu, E. Romão, D. Vertommen, C. Vincke, F. Morales-Yánez, C. Gutiérrez, C. Liu, S. Muyldermans, Generation of Nanobodies against *slyd* and development of tools to eliminate this bacterial contaminant from recombinant proteins, Protein Expr. Purif. 137 (2017) 64–76, https://doi.org/10.1016/j.pep.2017.06.016.
[18] S. Gelkop, A. Sobarzo, P. Brangel, C. Vincke, E. Romão, S. Fedida-Metula, N. Strom, I. Ataliba, F.N. Mwiine, S. Ochwo, L. Velazquez-Salinas, R.A. McKendry, S. Muyldermans, J.J. Lutwama, E. Rieder, V. Yavelsky, L. Lobel, The development and validation of a novel nanobody-based competitive elisa for the detection of Foot and Mouth Disease 3ABC antibodies in cattle, Front. Vet. Sci. 5 (2018) 1–13, https://doi.org/10.3389/fvets.2018.00250.
[19] M.M. Harmsen, H.J. De Haard, Properties, production, and applications of camelid single-domain antibody fragments, Appl. Microbiol. Biotechnol. 77 (2007) 13–22, https://doi.org/10.1007/s00253-007-1142-2.
[20] M. Arbabi Ghahroudi, A. Desmyter, L. Wyns, R. Hamers, S. Muyldermans, Selection and identification of single domain antibody fragments from camel heavy-chain antibodies, FEBS Lett. 414 (1997) 521–526, https://doi.org/10.1016/S0014-5793(97)01062-4.
[21] D. Ahmadvand, F. Rahbarizadeh, V.K. Vishteh, High-expression of monoclonal nanobodies used in the preparation of HRP-conjugated second antibody, Hybridoma 27 (2008) 269–276, https://doi.org/10.1089/hyb.2008.0006.
[22] P. Mason, A. Berinstein, B. Baxt, R. Parsells, A. Kang, E. Rieder, Cloning and expression of a single-chain antibody fragment specific for Foot-and-Mouth Disease virus, Virology 224 (1996) 548–554, https://doi.org/10.1006/viro.1996.0562.
[23] C. Vincke, C. Gutiérrez, U. Wernery, N. Devoogdt, G. Hassanzadeh-ghassabeh, S. Muyldermans, Generation of single domain antibody fragments derived from camelids and generation of manifold constructs, in: P. Chames (Ed.), Methods Mol. Biol., Humana Press, 2012, pp. 145–176, https://doi.org/10.1007/978-1-61779-974-7.
[24] V. Salema, L.Á. Fernández, High yield purification of Nanobodies from the periplasm of *E. coli* as fusions with the maltose binding protein, Protein Expr. Purif. 91 (2013) 42–48, https://doi.org/10.1016/j.pep.2013.07.001.
[25] B. Billen, C. Vincke, R. Hansen, N. Devoogdt, S. Muyldermans, P. Adriaensens, W. Guedens, Cytoplasmic versus periplasmic expression of site-specifically and bioorthogonally functionalized Nanobodies using expressed protein ligation, Protein Expr. Purif. 133 (2017) 25–34, https://doi.org/10.1016/j.pep.2017.02.009.
[26] F. Baneyx, Recombinant protein expression in *Escherichia coli*, Curr. Opin. Biotechnol. 10 (1999) 411–421, https://doi.org/10.1016/S0958-1669(99)00003-8.
[27] F. Baneyx, M. Mujacic, Recombinant protein folding and misfolding in *Escherichia coli*, Nat, Biotechnol. 22 (2004) 1399–1408, https://doi.org/10.1038/nbt1029.
[28] G. Ren, N. Ke, M. Berkmen, Use of the SHUffle strains in production of proteins, Curr. Protein Pept. Sci. (2016), https://doi.org/10.1002/cpps.11, 5.26.1-5.26.21.
[29] C.D. Martin, G. Rojas, J.N. Mitchell, K.J. Vincent, J. Wu, J. McCafferty, D. J. Schofield, A simple vector system to improve performance and utilisation of recombinant antibodies, BMC Biotechnol. 6 (2006) 1–15, https://doi.org/10.1186/1472-6750-6-46.
[30] J. Lobstein, C.A. Emrich, C. Jeans, M. Faulkner, P. Riggs, M. Berkmen, SHUffle, a novel *Escherichia coli* protein expression strain capable of correctly folding disulfide bonded proteins in its cytoplasm, Microb. Cell Factories 11 (2012) 1, https://doi.org/10.1186/1475-2859-11-56.
[31] M. Merdanovic, T. Clausen, M. Kaiser, R. Huber, M. Ehrmann, Protein quality control in the bacterial periplasm, Annu. Rev. Microbiol. 65 (2011) 149–168, https://doi.org/10.1146/annurev-micro-090110-102925.
[32] H. Kadokura, J. Beckwith, Mechanisms of oxidative protein folding in the bacterial cell envelope, Antioxidants Redox Signal. 13 (2010) 1231–1246, https://doi.org/10.1089/ars.2010.3187.
[33] H. Kadokura, F. Katzen, J. Beckwith, Protein disulfide bond formation in prokaryotes, Annu. Rev. Biochem. 72 (2003) 111–135, https://doi.org/10.1146/annurev.biochem.72.121801.161459.
[34] J. De Keyzer, C. Van Der Does, A.J.M. Driessen, The bacterial translocase: a dynamic protein channel complex, Cell. Mol. Life Sci. 60 (2003) 2034–2052, https://doi.org/10.1007/s00018-003-3006-y.
[35] J.A. Lycklama a Nijeholt, A.J.M. Driessen, The bacterial *sec*-translocase: structure and mechanism, Philos. Trans. R. Soc. B Biol. Sci. 367 (2012) 1016–1028, https://doi.org/10.1098/rstb.2011.0201.
[36] D.J.F. Du Plessis, N. Nouwen, A.J.M. Driessen, The *sec* translocase, Biochim. Biophys. Acta Biomembr. 1808 (2011) 851–865, https://doi.org/10.1016/j.bbamem.2010.08.016.
[37] G. Lee, P A, Tullman-Ercek, D. Georgiou, The bacterial twin-arginine translocation pathway, Biochim. Biophys. Acta Biomembr. 1778 (2006) 373–395, https://doi.org/10.1146/annurev.micro.60.080805.142212.
[38] D. Steiner, P. Forrer, M.T. Stumpp, A. Plückthun, Signal sequences directing cotranslational translocation expand the range of proteins amenable to phage display, Nat. Biotechnol. 24 (2006) 823–831, https://doi.org/10.1038/nbt1218.
[39] P. Singh, L. Sharma, S.R. Kulothungan, B.V. Adkar, R.S. Prajapati, P.S.S. Ali, B. Krishnan, R. Varadarajan, Effect of signal peptide on stability and folding of *Escherichia coli* thioredoxin, PloS One 8 (2013), https://doi.org/10.1371/journal.pone.0063442.
[40] A. De Marco, Recombinant expression of nanobodies and nanobody-derived immunoreagents, Protein Expr. Purif. 172 (2020), https://doi.org/10.1016/j.pep.2020.105645.
[41] N.G. Nossal, L.A. Heppel, The release of enzymes by osmotic shock from *Escherichia coli* in exponential phase, J. Biol. Chem. 241 (1966) 3055–3062, https://doi.org/10.1016/s0021-9258(18)96497-5.
[42] H.C. Neu, L.A. Heppel, The release of enzymes from *Escherichia coli* by osmotic shock and during the formation of spheroplasts, J. Biol. Chem. 240 (1965) 3685–3692, https://doi.org/10.1016/s0021-9258(18)97200-5.
[43] N. Vázquez-Laslop, H. Lee, R. Hu, A.A. Neyfakh, Molecular sieve mechanism of selective release of cytoplasmic proteins by osmotically shocked *Escherichia coli*, J. Bacteriol. 183 (2001) 2399–2404, https://doi.org/10.1128/JB.183.8.2399-2404.2001.
[44] E. Pardon, T. Laeremans, S. Triest, S.G.F.F. Rasmussen, A. Wohlkönig, A. Ruf, S. Muyldermans, W.G.J.J. Hol, B.K. Kobilka, J. Steyaert, A general protocol for the generation of Nanobodies for structural biology, Nat. Protoc. 9 (2014) 674–693, https://doi.org/10.1038/nprot.2014.039.
[45] U.K. Laemmli, Cleavage of structural proteins during the assembly of the head of bacteriophage T4, Nature 227 (1970) 680–685, https://doi.org/10.1038/227680a0.
[46] H. Towbin, T. Staehelin, J. Gordon, J. Ross, Electrophoretic transfer of proteins from polyacrylamide gels to nitrocellulose sheets: procedure and some applications, Proc. Natl. Acad. Sci. U. S. A. 76 (1979) 4350–4354, https://doi.org/10.1002/bies.950190612.
[47] F.H. Niesen, H. Berglund, M. Vedadi, The use of differential scanning fluorimetry to detect ligand interactions that promote protein stability, Nat. Protoc. 2 (2007) 2212–2221, https://doi.org/10.1038/nprot.2007.321.
[48] M. Ruiz, M.P. Lefranc, IMGT gene identification and Colliers de Perles of human immunoglobulins with known 3D structures, Immunogenetics 53 (2002) 857–883, https://doi.org/10.1007/s00251-001-0408-6.
[49] Q. Kaas, M.-P. Lefranc, IMGT Colliers de Perles: standardized sequence-structure representations of the IgSF and MHCSF superfamily domains, Curr. Bioinf. 2 (2007) 21–30, https://doi.org/10.2174/157489307779314302.
[50] Q. Kaas, M. Ruiz, M.P. Lefranc, IMGT/3Dstructure-DB and IMGT/StructuralQuery, a database and a tool for immunoglobulin, T cell receptor and MHC structural data, Nucleic Acids Res. 32 (2004), https://doi.org/10.1093/nar/gkh042.
[51] V. Lejon, D. Legros, M. Richer, J.A. Ruiz, V. Jamonneau, P. Truc, F. Doua, N. Djé, F. X. N'Siesi, S. Bisser, E. Magnus, I. Wouters, J. Konings, T. Vervoort, F. Sultan, P. Büscher, IgM quantification in the cerebrospinal fluid of sleeping sickness patients by a latex card agglutination test, Trop. Med. Int. Health 7 (2002) 685–692, https://doi.org/10.1046/j.1365-3156.2002.00917.x.
[52] M.P. Lefranc, C. Pommié, Q. Kaas, E. Duprat, N. Bosc, D. Guiraudou, C. Jean, M. Ruiz, I. Da Piédade, M. Rouard, E. Foulquier, V. Thouvenin, G. Lefranc, IMGT unique numbering for immunoglobulin and T cell receptor constant domains and Ig superfamily C-like domains, Dev. Comp. Immunol. 29 (2005) 185–203, https://doi.org/10.1016/j.dci.2004.07.003.
[53] S. Muyldermans, C. Vincke, Structure and function of camelid VHH, Encycl. Immunobiol. 2 (2016) 153–159, https://doi.org/10.1016/B978-0-12-374279-7.05019-0.
[54] E. Gasteiger, C. Hoogland, A. Gattiker, S. Duvaud, M.R. Wilkins, R.D. Appel, A. Bairoch, Protein identification and analysis tools on the expasy server, Proteomics Protoc. Handb (2005) 571–607, https://doi.org/10.1385/1592598900.
[55] S. Muyldermans, T.N. Baral, V.C. Retamozzo, P. De Baetselier, E. De Genst, J. Kinne, H. Leonhardt, S. Magez, V.K. Nguyen, H. Revets, U. Rothbauer, B. Stijlemans, S. Tillib, U. Wernery, L. Wyns, G. Hassanzadeh-Ghassabeh, D. Saerens, Camelid immunoglobulins and Nanobody technology, Vet. Immunol.

Immunopathol. 128 (2009) 178–183, https://doi.org/10.1016/j.vetimm.2008.10.299.
[56] T. De Meyer, S. Muyldermans, A. Depicker, Nanobody-based products as research and diagnostic tools, Trends Biotechnol. 32 (2014) 263–270, https://doi.org/10.1016/j.tibtech.2014.03.001.
[57] A. Tsirigotaki, J. De Geyter, N. Šoštaric, A. Economou, S. Karamanou, Protein export through the bacterial *sec* pathway, Nat. Rev. Microbiol. 15 (2016) 21–36, https://doi.org/10.1038/nrmicro.2016.161.
[58] B.E. Power, N. Ivancic, V.R. Harley, R.G. Webster, A.A. Kortt, R.A. Irving, P. J. Hudson, High-level temperature-induced synthesis of an antibody VH-domain in *Escherichia coli* using the *pelB* secretion signal, Gene 113 (1992) 95–99, https://doi.org/10.1016/0378-1119(92)90674-E.
[59] H.N. Ananthaswamy, The release of endonuclease I from *Escherichia coli* by a new cold shock procedure, Biochem. Biophys. Res. Commun. 76 (1977) 289–298, https://doi.org/10.1016/0006-291x(77)90724-0.